Control of Spatiotemporal Disorder in Parametrically Excited Surface Waves

T. Epstein and J. Fineberg

The Racah Institute of Physics, The Hebrew University of Jerusalem, Jerusalem 91904, Israel

(Received 21 August 2003; revised manuscript received 13 January 2004; published 15 June 2004)

Interacting surface waves, parametrically excited by two commensurate frequencies, yield a number of nonlinear states. Near the system's bicritical point, a state, highly disordered in space and time, results from competition between nonlinear states. Experimentally, this disordered state can be rapidly stabilized to a variety of nonlinear states via open-loop control with a small-amplitude third frequency excitation, whose temporal symmetry governs the temporal and the spatial symmetry of the selected nonlinear state. This technique also excites rapid switching between nonlinear states.

DOI: 10.1103/PhysRevLett.92.244502 PACS numbers: 47.54.+r, 05.45.Gg, 47.27.Rc, 52.35.Mw

A driven nonlinear system can have a multiplicity of possible solutions, which we define as nonlinear states. Examples range from temporally chaotic systems, where an infinite number of unstable periodic orbits exists, to turbulent states in which myriad unstable modes, which exhibit disordered behavior in both space and time, coexist within the flow. An important question is whether one can control a highly disordered system that possesses multiple spatial as well as temporal degrees of freedom. Parametrically excited waves in a large, spatially extended system can directly bifurcate from a trivial state to a highly disordered one. We will first show that this disorder is intrinsic and results from competition between different families of nonlinear states. By imposing a small-amplitude control frequency, we will achieve both control of this state and force rapid transitions between different, stabilized, nonlinear states.

Over the past decade, a large amount of work has been invested in the taming of temporally chaotic systems. The control schemes proposed can roughly be divided into two general classes: closed-loop and open-loop control. Closed-loop control of unstable states is achieved by continuous feedback that is applied near either hyperbolic fixed points [1] or pinning sites [2] within a system. Closed-loop stabilization of a system necessitates detailed knowledge of its phase space, constant feedback, and the technical ability to apply the desired control.

Open-loop control [3] is performed by perturbation with an external forcing frequency. Here, no feedback is needed and, therefore, detailed knowledge of the phase space is not required. Successful open-loop control has been achieved in temporal systems [4] and some model systems [3] but, to our knowledge, has not been experimentally demonstrated in spatially extended disordered systems.

Our experiments describe forced nonlinear waves on the 2D surface of a fluid. The uncontrolled system is driven by a spatially uniform, temporally periodic vibration of the fluid layer of the form $a_{\mathrm{H}}\cos(2n_e\omega_0 t) + a_{\mathrm{SH}}\cos(2n_o\omega_0 t + \phi)$, where n_o, n_e are mutually prime, odd and even integers [5]. The experiments were performed in a 150 mm diameter cell filled with 20 cS silicon oil at $30.5 \pm 0.05\,^{\circ}\mathrm{C}$, $\omega_0/2\pi = 6$ Hz, and a fluid depth of 0.11 cm. The bulk of our quantitative measurements were performed at the frequency ratio $n_e/n_o = \frac{4}{5}$ and $\phi = 0$, although the same qualitative behavior occurred for frequency ratios $\frac{2}{3}$, $\frac{6}{7}$, $\frac{8}{9}$, $\frac{6}{5}$, and $\frac{8}{7}$. Details of both the experimental system and phase diagram can be found in [6,7].

The temporal response of the system's linearly unstable modes can either be *even* ("harmonic") or *odd* ("subharmonic") multiples of ω_0 [5,8]. We denote a_{H} and a_{SH}, respectively, as the driving amplitudes of the harmonic and subharmonic frequencies. The wave numbers, k_{H} and k_{SH}, of these modes are determined by the dispersion relation and the dominant response frequencies $\omega_{\mathrm{H}} = n_e\omega_0$ and $\omega_{\mathrm{SH}} = n_o\omega_0$. For any set of system parameters, a critical mixing angle, χ_c [$\chi \equiv a\tan(a_{\mathrm{SH}}/a_{\mathrm{H}})$] exists where both k_{H} and k_{SH} simultaneously lose stability.

As shown in Fig. 1(a), a variety of both ordered and highly disordered nonlinear states exist within a small region of phase space surrounding χ_c [5–7,9]. These states are characterized by different spatial as well as temporal symmetries [10]. In this vicinity, standing wave patterns corresponding to four different nonlinear states

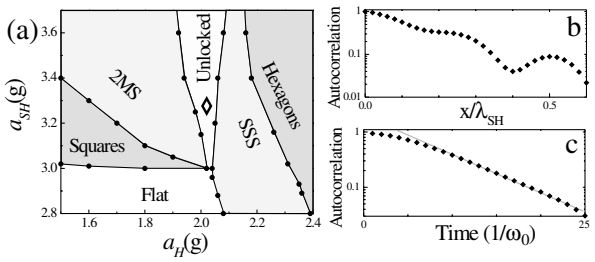

FIG. 1. (a) An enlarged view of the phase space surrounding $\chi_c = 55.8°$, with $\omega_{\mathrm{SH}} = 5\omega_0$, $\omega_{\mathrm{H}} = 4\omega_0$, $h = 0.11$ cm, and $\nu = 20$ cS. Correlation functions in (b) space (scaled by $\lambda_{\mathrm{SH}} = 2\pi/k_{\mathrm{SH}}$) and (c) time of a typical unlocked state [located at $\diamond$ in (a)] exhibit the exponential decay characteristic of spatiotemporal chaos. The internal structure for $x < \lambda_{\mathrm{SH}}$ leads to the oscillations in (b).

 0031-9007/04/92(24)/244502(4)$22.50

are observed: two-mode superlattices (2MS), subharmonic superlattice states (SSS) [6], hexagonal states, and a highly disordered state, defined as the unlocked state. The 2MS states [6] are formed by the resonant triads $\vec{k}_{\mathrm{SH}} - \vec{k}_{\mathrm{H}} = \vec{k}_{\mathrm{diff}}$, where k_{diff} is the wave number corresponding to a linearly stable mode excited at the frequency $\omega_{\mathrm{SH}} - \omega_{\mathrm{H}}$. The hexagonal states are composed of only k_{H} modes, whereas the SSS states are superlattice patterns composed of only $\vec{k}_{\mathrm{H}}$ and linearly stable spatial subharmonics, $\vec{k}_{\mathrm{H}}/2$. In the phase space presented in Fig. 1(a), both 2MS and SSS states have an overall 90° spatial symmetry, although in general these states can have either a 90° or a 60° spatial symmetry. The essential difference between these states is in both the spatial resonances and the temporal characteristics of the linear modes needed to construct them.

The parity of n_e (n_o) is important in determining both the temporal character of the linear modes and their allowed nonlinear couplings to other modes [10]. Slaved modes, i.e., linearly stable modes (e.g., $k_{\mathrm{H}}/2$ and k_{diff}) which are excited by nonlinear coupling to excited ones, are critical in determining the resultant nonlinear state. On either side of χ_c, the parity of the dominant linear mode needed to construct a given state is well defined; 2MS states by the temporally *subharmonic* k_{SH} mode, and both the SSS state and hexagonal state by the *harmonically* excited k_{H} modes.

The unlocked state is a nonlinear state with a high degree of disorder in both space and time. This state bifurcates directly from the featureless state via a continuous transition. Despite its close proximity to ordered states, the unlocked phase exhibits exponentially decaying correlations in both space [Fig. 1(b)] and time [Fig. 1(c)]. The values of both the decay time and length are dependent on the phase space location. Correlations rapidly decay by typically 2 orders of magnitude within an either single wavelength (in space) or $\sim 10/\omega_0$ (in time). Such exponential decay in both space and time are defining characteristics of spatiotemporal chaos (STC). STC occurs in many driven nonlinear systems, but it is clear that different classes of such disordered states may exist. A more precise characterization of these states is crucial both for understanding and intelligently "controlling" them.

To quantify the degree of symmetry of a wave number k within a given state, we use the angular correlation function [6,11], $C_k(\theta)$, defined as

$$C_k(\theta) = \sum_{\alpha} [(f_k(\theta) - \bar{f}_k)(f_k(\theta + \alpha) - \bar{f}_k)] \Big/ \sum_{\alpha} [(f_k(\alpha) - \bar{f}_k)^2],$$

where $f_k(\theta)$ is the 2D spatial Fourier transform of the state at *specific* values of k and the angle θ. $\bar{f}_k$ is the mean value of $f_k(\theta)$, averaged over θ. Maximal values of $C_k(\theta)$ are thereby normalized to 1. The unlocked state exhibits negligible angular correlations at all wave numbers [6], whereas the neighboring phases are characterized by a high degree of correlation at all excited values of k.

Let us consider the transition from the ordered 2MS state, characterized by a high degree of 90° symmetry, to the unlocked phase. Figure 2(a) shows that the mean values of both $C_{k_{\mathrm{SH}}}(90°)$ and $C_{k_{\mathrm{H}}}(90°)$ continuously decrease from a high degree of correlation ($C_{k_{\mathrm{SH}}}(90°) > 0.6$) to near zero as the boundary of the unlocked state [defined at $\epsilon \equiv (a_{\mathrm{H}} - a_{\mathrm{H}_c})/a_{\mathrm{H}_c} = 0$] is approached.

To understand the mechanism that drives this rapid loss of correlation, we compare [Fig. 2(b) (top panels)] the temporal behaviors of $C_{k_{\mathrm{SH}}}(90°)$ and $C_{k_{\mathrm{H}}}(60°)$ as $\epsilon \to 0$. $C_{k_{\mathrm{SH}}}(90°)$ [$C_{k_{\mathrm{H}}}(60°)$] is representative of the subharmonic 2MS (harmonic hexagonal) state. Relatively far from the unlocked phase boundary, $C_{k_{\mathrm{SH}}}(90°)$ indicates a high degree of square symmetry with rare momentary losses of correlation. As the phase boundary is approached, the frequency of these dips in correlation increases with a corresponding decrease in the mean value of $C_{k_{\mathrm{SH}}}(90°)$. Surprisingly, the momentary losses of correlation represented by $C_{k_{\mathrm{SH}}}(90°)$ correspond to momentary *growth* of $C_{k_{\mathrm{H}}}(60°)$. The anticorrelated behavior of the two functions is quantified by their cross-correlation functions [Fig. 2(b) (bottom panels)]. The degree of anticorrelation [Fig. 2(c)] first increases in the transition region as $\epsilon \to 0^-$, until, near $\epsilon = 0$, the cross-correlation function goes to zero, as all angular correlations vanish within the unlocked phase.

We may now understand the disorder characterizing the unlocked phase as resulting from continual competition between the hexagonal and SSS states (dominated by the temporally harmonic k_{H} modes) with the temporally subharmonic 2MS states. As the phase boundary is approached, the intermittent behavior characterizing the loss of coherence of the 2MS state results from intermittent switching between these nonlinear states, each with its own distinct temporal and spatial symmetries. Finally, once within the unlocked phase, neither state is dominant thereby giving rise to a regime (the unlocked phase) that possesses *no* temporal or spatial symmetry.

Let us now attempt to control this state. As in [7,12], where the addition of a third frequency perturbation was seen to influence pattern stability, we add a small-amplitude, spatially uniform control signal, $a_\Omega \cos(2\Omega t)$, to the forcing function. We consider values of a_Ω that are significantly smaller than $a_{\Omega_{\mathrm{crit}}}$, the value of a_Ω where a flat state loses stability when driven at a single frequency of 2Ω. This perturbation will break the degeneracy of the competing states but will not add new states to the phase diagram in Fig. 1(a). The perturbation frequency, Ω, is chosen to be either an odd or an even multiple of ω_0. Since the allowed (triad) nonlinear interactions conserve parity

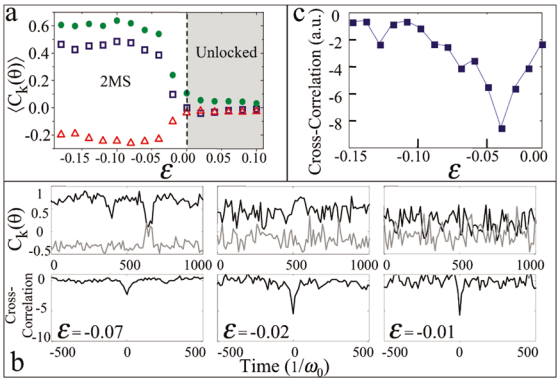

FIG. 2 (color online). The transition from the ordered (2MS) state to the disordered unlocked state for a fixed value $a_{\mathrm{SH}} = 3.4g$. (a) Time averaged angular correlation functions, $C_k(\theta)$, as a function of the distance $\epsilon \equiv (a_{\mathrm{H}} - a_{\mathrm{H}_c})/a_{\mathrm{H}_c}$ from the transition value a_{H_c} of the harmonic driving acceleration, a_{H}. The 90° correlation amplitudes of the two coupled wave numbers (●) $C_{k_{\mathrm{SH}}}(90°)$ and (□) $C_{k_{\mathrm{H}}}(90°)$ decrease while the correlation amplitude, $C_{k_{\mathrm{H}}}(60°)$ (△), indicating hexagonal symmetry of k_{H} increases as $\epsilon \rightarrow 0$. (b) (top panels) The frequency and size of fluctuations increase both in $C_{k_{\mathrm{SH}}}(90°)$ (black line) and $C_{k_{\mathrm{H}}}(60°)$ (grey line) as $\epsilon \rightarrow 0$. The respective cross-correlation functions (bottom panels) indicate that the fluctuations of $C_{k_{\mathrm{SH}}}(90°)$ and $C_{k_{\mathrm{H}}}(60°)$ are anticorrelated. (c) The peak values of the cross-correlation coefficients increase as the unlocked state is approached.

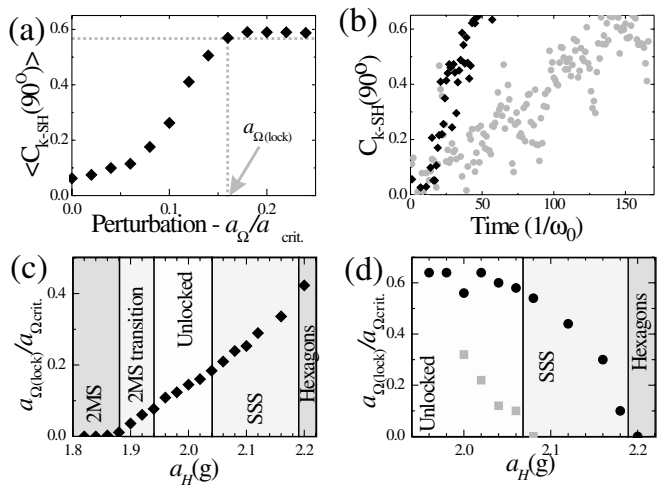

FIG. 3. (a) Control of a typical unlocked state (at $a_{\mathrm{SH}} = 3.4g$, $a_{\mathrm{H}} = 2g$) to the 2MS state is achieved at a perturbation amplitude of $a_{\Omega(\mathrm{lock})} = 0.16a_{\Omega\mathrm{crit}}$ with $\Omega = \omega_0$ ($a_{\Omega\mathrm{crit}} = 1.5g$). $a_{\Omega_{lock}}$ is the value of a_Ω at which temporally averaged, $\langle C_k(90°)\rangle$, reaches the value of C_k characteristic of a stable 2MS state. (b) The time to stabilize the unlocked state is a decreasing function of $a_\Omega/a_{\Omega_{\mathrm{lock}}}$. Typical examples of the temporal evolution of $C_k(90°)$ for $\Omega = \omega_0$ and $a_\Omega = a_{\Omega_{\mathrm{lock}}}$ (squares) and $a_\Omega = 2a_{\Omega_{\mathrm{lock}}}$ (circles) where both experiments were initiated at $a_\Omega = 0$ from the same unlocked state. Values of $a_{\Omega(\mathrm{lock})}$ needed to stabilize the (c) 2MS state ($\Omega = \omega_0$) and (d) the SSS state (squares) and hexagonal state (circles) (where $\Omega = 2\omega_0$, $a_{\Omega\mathrm{crit}} = 1.6g$) as a_{SH} is fixed at $3.4g$ and a_{H} is varied across the four different phases. In both (c) and (d), stabilization of each state is achieved within the region of phase space where competing nonlinear states are stable.

[10,13], the parity of Ω should boost only selected linear modes. By enhancing selected dominant modes, we expect to favor different nonlinear interactions and thereby choose a desired nonlinear state. Roughly, choosing Ω to be an odd (even) multiple of ω_0 should induce the selection of a subharmonic (k_{H} dominated) state.

Successful control of the unlocked phase to both harmonic and subharmonic states is demonstrated in Fig. 3. Let us first consider the application of $\Omega = \omega_0$. Starting from an initially unlocked state, the degree of correlation of the state as a function of a_Ω is measured. The correlation amplitude of the system continuously increases [Fig. 3(a)] with a_Ω, reaching a plateau at values of $C_k(90°) \sim 0.6$ characteristic of the k_{SH}-dominated 2MS state. We define the locking amplitude, $a_{\Omega_{\mathrm{lock}}}$, as the value of a_Ω at which $C_k(\theta)$ reaches the level attained by a stable nonlinear state. As Fig. 3(c) demonstrates, 2MS stabilization can be achieved for small values of $a_\Omega/a_{\Omega_{\mathrm{crit}}}$, increasing nearly linearly from $a_\Omega/a_{\Omega_{\mathrm{crit}}} = 0$ at the 2MS-unlocked phase boundary to about 0.3 at the hexagonal phase boundary. Application of $a_{\Omega_{\mathrm{lock}}} \sim 0.4a_{\Omega_{\mathrm{crit}}}$ enables stabilization of the 2MS state well into the hexagonal phase.

A harmonic perturbation [$\Omega = 2\omega_0$ in Fig. 3(d)] will stabilize both the harmonic k_{H}-dominated hexagonal and the SSS states. The perturbation amplitude necessary for stabilizing the unlocked to the SSS states increases continuously from zero, at the SSS-unlocked phase boundary to about $0.3a_{\Omega_{\mathrm{crit}}}$ near the 2MS phase boundary. Within this regime, increase of a_Ω can force a transition from the SSS to the hexagonal states.

As in the case of the subharmonic perturbations, harmonic perturbations can stabilize the harmonic hexagonal states in regions that are well within the subharmonic 2MS phase. It is interesting to note that, in contrast to the nearly linear dependence of $a_{\Omega_{\mathrm{lock}}}$ for odd values of Ω with the distance from the subharmonic phase, a highly nonlinear dependence of $a_{\Omega_{\mathrm{lock}}}$ on the distance from the hexagonal and SSS phases is evident for $\Omega_{\mathrm{lock}} = 2\omega_0$. Besides achieving control with $\Omega = \omega_0$ and $\Omega = 2\omega_0$, selection of 2MS (SSS and hexagonal) states has also been achieved with $\Omega = 3\omega_0$ and $5\omega_0$ ($\Omega = 4\omega_0$) for a number of different frequency ratios.

When control is applied to the unlocked state, on average, the speed of stabilization is an increasing function of $a_\Omega/a_{\Omega_{\mathrm{lock}}}$. This is demonstrated for two typical cases in Fig. 3(b). The stabilization time for a given instance, however, is highly dependent on initial conditions, and the variance around the mean stabilization time is large. Although initial stabilization to a finite number of domains is rapid (within $\sim\omega_0^{-1}$), the time needed for high [$C_{k_{\mathrm{SH}}}(90°) > 0.6$] spatial correlation throughout the entire system is highly dependent on the initial configuration of the system at the time of control application, and

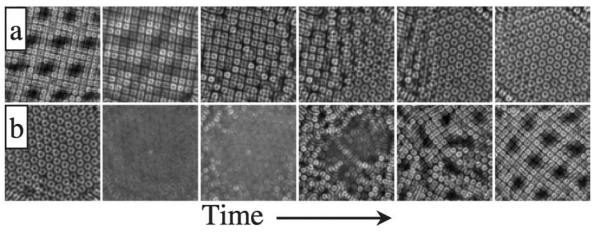

FIG. 4. Patterns can be rapidly controlled by switching perturbation frequencies. Typical transitions from (a) 2MS to hexagonal states as Ω is switched from ω_0 to $2\omega_0$ at times $(0, 2, 4, 30, 100)\omega_0^{-1}$ and (b) hexagonal to a 2MS state as Ω is switched from $2\omega_0$ to ω_0 at times $(0, 1, 40, 60, 100)\omega_0^{-1}$. Time progresses from left to right. In both transitions, the dominant wave number changes within $1\omega_0^{-1}$, although the final state evolves via domain coarsening in (a) and front propagation in (b) over much longer times.

the subsequent dynamics of domain coalescence. Such domain formation is demonstrated in Fig. 4(b).

As demonstrated in Fig. 4, this method can be used for rapid switching between different nonlinear states by switching the temporal parity of Ω. Switching the parity from odd to even will cause a transition from an initial (odd-parity) 2MS state to the even-parity hexagonal state, whereas application of odd-parity control forces the reverse transition. When the transition is to the even-parity state, the initial state is first erased immediately upon application of the control signal [Fig. 4(b), second frame], with the new pattern appearing within a time $t \sim \omega_0^{-1}$ with the wave number corresponding to the even-parity state. When an odd-parity driven transition is forced, no such erasure occurs but the dominant wave number [Fig. 4(a), second frame] is *replaced* by that of the controlled state within a time $\sim\omega_0^{-1}$. The subsequent dynamics of the transitions are governed by both the initial conditions at $t = 0$ and the parity of the new nonlinear state. For $\frac{4}{5}$ forcing, when the new state has even parity, the system's initial state is generally a SSS state. This state will then evolve to a hexagonal state, where the long-time dynamics of the transition are governed by a front propagating from the SSS into the hexagonal state [see frames 4 and 5 of Fig. 4(a)]. On the other hand, when an initial hexagonal state is forced to a 2MS state, a number of 2MS domains are immediately formed, and the long-time dynamics of the transition are governed by domain coarsening [Fig. 4(b)].

In conclusion, we have first shown that the mechanism driving the spatiotemporal disorder in this system is the continual competition between a number of specific nonlinear states. Within this disordered regime, standard diagnostics, such as spatial, temporal, or orientational correlation functions, provide no hint of the underlying reasons for this complexity. Only when control of this regime is applied can we successfully identify the building blocks that give rise to this highly disordered regime. This work may elucidate the mechanisms driving other, currently not understood, types of spatiotemporal disorder (e.g., "domain chaos" [14]) that occur as primary bifurcations of nonlinear systems.

We have shown further that symmetries (e.g., the temporal parity) of nonlinear systems can be used for both open-loop control of this type of spatiotemporal disorder and selection of desired nonlinear states in large, spatially extended systems. These ideas should be applicable to other parametrically excited systems (e.g., [15]). It may also be possible to extend the method by matching the perturbing frequency to different slaved modes, thereby efficiently selecting different (like-parity) nonlinear states which are coupled to these modes [13].

This research was supported by the Israel Science Foundation (Grant No. 194/02).

[1] See, e.g., E. Ott, C. Grebogi, and J. A. Yorke, Phys. Rev. Lett. **64**, 1196 (1990); S. D. Pethel, N. J. Corron, Q. R. Underwood, and K. Myneni, Phys. Rev. Lett. **90**, 254101 (2003); S. Boccaletti *et al.*, Phys. Rep. **329**, 103 (2000).

[2] R. O. Grigoriev, M. C. Cross, and H. G. Schuster, Phys. Rev. Lett. **79**, 2795 (1997); P. Kolodner, G. Flatgen, and I. G. Kevrekidis, Phys. Rev. Lett. **83**, 730 (1999).

[3] Y. Braiman and I. Goldhirsch, Phys. Rev. Lett. **66**, 2545 (1991); R. Lima and M. Pettini, Phys. Rev. A **41**, 726 (1990); V. V. Alexeev and A. I. Loskutov, Dokl. Akad. Nauk SSSR **293**, 1346 (1987); Y. S. Kivshar, F. Rodelsperger, and H. Benner, Phys. Rev. E **49**, 319 (1994); S. Wu, K. He, and Z. Huang, Phys. Rev. E **62**, 4417 (2000).

[4] A. Seifert and L. G. Pack, J. Aircraft **38**, 464 (2001).

[5] W. S. Edwards and S. Fauve, Phys. Rev. E **47**, R788 (1993); J. Fluid Mech. **278**, 123 (1994).

[6] H. Arbell and J. Fineberg, Phys. Rev. Lett. **81**, 4384 (1998); Phys. Rev. Lett. **84**, 654 (2000).

[7] H. Arbell and J. Fineberg, Phys. Rev. E **65**, 036224 (2002).

[8] T. Besson, W. S. Edwards, and L. S. Tuckerman, Phys. Rev. E **54**, 507 (1996).

[9] A. Kudrolli and J. P. Gollub, Physica (Amsterdam) **97D**, 133 (1996).

[10] M. Silber and A. C. Skeldon, Phys. Rev. E **59**, 5446 (1999); J. Porter and M. Silber, Phys. Rev. Lett. **89**, 084501 (2002); C. M. Topaz and M. Silber, Physica (Amsterdam) **172D**, 1 (2002); D. P. Tse, A. M. Rucklidge, R. B. Hoyle, and M. Silber, Physica (Amsterdam) **146D**, 367 (2000).

[11] F. Simonelli and J. P. Gollub, J. Fluid Mech. **199**, 471 (1989); D. Binks and W. van de Water, Phys. Rev. Lett. **78**, 4043 (1997).

[12] H. W. Muller, Phys. Rev. Lett. **71**, 3287 (1993).

[13] J. Porter, C. M. Topaz, and M. Silber, arXiv:nlin.PS/0307056.

[14] E. Bodenschatz, W. Pesch, and G. Ahlers, Annu. Rev. Fluid Mech. **32**, 709 (2000); M. C. Cross, M. Louie, and D. Meiron, Phys. Rev. E **63**, 045201 (2001); M. Silber and A. C. Skeldon, Phys. Rev. E **59**, 5446 (1999).

[15] P. Colet and Y. Braiman, Phys. Rev. E **53**, 200 (1996).